



Experimental investigation of deficient RC frames retrofitted by RSFJ-toggle bracing systems

Sajad Veismoradi^{a,*}, Seyed Mohamad Mahdi Yousef-beik^a, Pouyan Zarnani^a,
Pierre Quenneville^b

^a Department of Built Environment Engineering, Auckland University of Technology, New Zealand

^b Department of Civil and Environmental Engineering, The University of Auckland, New Zealand

ARTICLE INFO

Keywords:

Global retrofitting
Pre-1970 RC frames
Self-centring
Toggle-bracing
Stability

ABSTRACT

This paper investigates the performance of the new retrofitting system, consisting of self-centring damper resilient slip friction joint (RSFJ)-toggle bracing system. The RSFJ-toggle bracing system can be activated within small drift values of the frame and preserve the frame from excessive damage. Two scaled deficient RC frames representing typical pre-1970s RC moment resisting frames were constructed and tested to investigate the performance of such retrofitting system. Material testing of the concrete and steel rebars as well as the damper component testing were conducted and recommendations regarding the proper design of various aspects of this retrofitting system were provided. The experimental observations demonstrate the improved behaviour of the frame in terms of energy dissipation and enhanced stiffness and strength for the upgraded RC frame. As per the findings of this study, the proposed retrofit solution can strengthen the frames within a limited drift and improve the frame's damping with a repeatable semi-flag shape hysteresis performance.

1. Introduction

A reinforced Concrete (RC) building structure should have sufficient strength, stiffness and ductility to perform well during major seismic events. A high number of existing RC buildings, especially those built prior to 1970s might not satisfy the current seismic codes criteria, due to the fact that they are mainly designed based on gravity load only [1], and lack the seismic detailing required for lateral loads and deformations imposed during high seismic events. The need for practical retrofitting techniques still remains as an important topic within the structural engineering community.

Depending on the required level of seismic retrofitting, the deficient RC structures may go through a member-level upgrading (local-retrofitting), or structural-level upgrading (global-retrofitting) [2]. Examples of local retrofitting includes addition of various jackets [3,4] or structural haunches to the beam-column joints [5], whereas the global retrofitting methods include shear-walls or various types of steel braces to the RC frame to reduce storey drifts and ductility demand [6].

Besides utilising traditional global retrofitting methods, researchers have also explored the possibility of using innovative seismic dampers for seismic upgrading of RC frames [7]. Javidan and Kim [8–10]

introduced a system consisting of pin-jointed steel frame with rotational-friction damper for design and seismic retrofitting of a fragile RC frame with soft-storey issue. In another study, Javidan et al. [11] presented a steel hysteretic column damper for seismic retrofitting of RC structures and tested the damper on a single-story one-bay RC frame. Such a damper has the benefits of occupying only a small space next to the column without blocking the passage of people or vehicles.

Eskandari Nasab et al. [12] employed Visco-Elastic Dampers (VEDs) with fail-safe mechanism for retrofitting of a full-scale two-story RC frame and studied the performance of such dampers in terms of inter-storey and residual drift reduction. Tahamouli Roudsari et al. [13] performed an experimental testing on seven RC frames where six of them were retrofitted by chevron bracing with different numbers of ADAS and TADAS yielding dampers. Their results showed that the dampers increase the strength of the RC frames, as well as ductility, energy dissipation and strength reduction factor for all the frames. Sarno and Manfredi [14] investigated the applications of Buckling Restrained Braces (BRBs) as hysteretic energy dissipation elements for seismic retrofitting of a typical two-story gravity-only RC frame. Their results showed the concentration of damage in the BRBs while the existing RC frame remained elastic. Vafaei et al. [15] experimentally investigated a

* Corresponding author.

E-mail address: Sajad.Veismoradi@aut.ac.nz (S. Veismoradi).

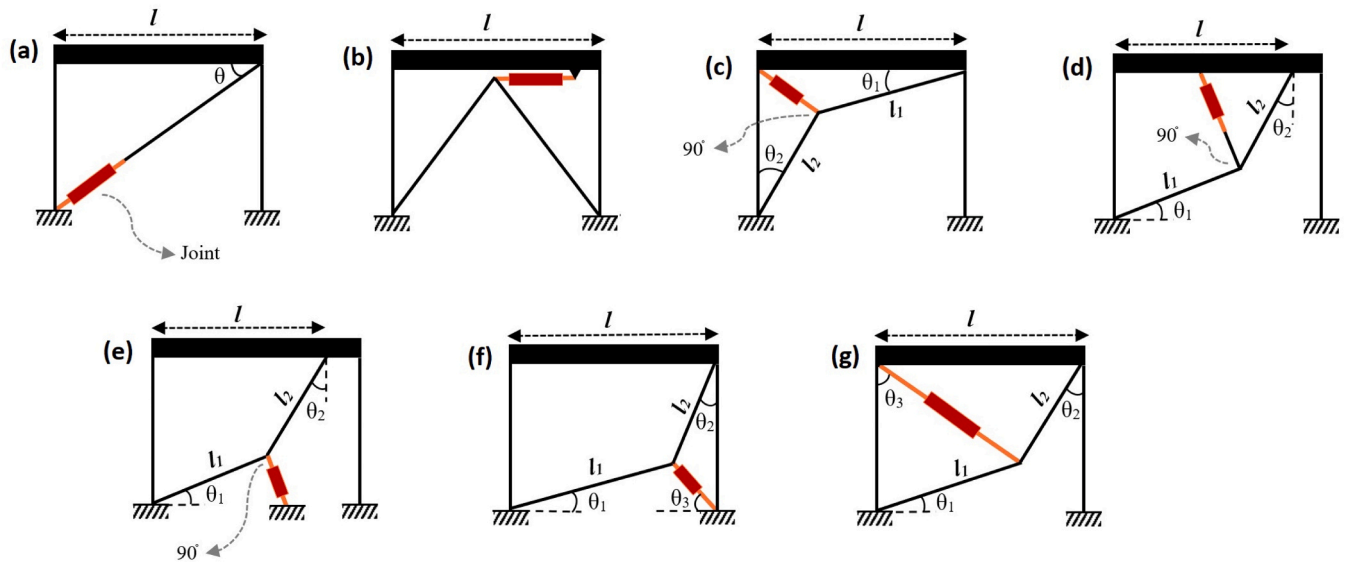


Fig. 1. Schematic view of different toggle-bracing arrangement, as compared to common bracing systems.

Table 1
Amplification factor for different bracing system [18,19].

System ID	Name	Amplification factor (f)
a	Diagonal	$\cos\theta$
b	Chevron	1.0
c	Reverse Toggle	$\frac{\cos\theta_1}{\cos(\theta_1 + \theta_2)} - \cos\theta_2$
d	Upper Toggle (Type I)	$\frac{\sin\theta_2}{\cos(\theta_1 + \theta_2)} + \sin\theta_1$
e	Lower Toggle (Type I)	$\frac{\sin\theta_2}{\cos(\theta_1 + \theta_2)}$
f	Lower Toggle (Type II)	$\frac{\sin\theta_2 \sin(\theta_1 + \theta_3)}{\cos(\theta_1 + \theta_2)}$
g	Upper Toggle (Type II)	$\frac{\sin\theta_2}{\cos(\theta_1 + \theta_2)} \cos(\theta_3 - \theta_1) + \sin\theta_3$

specific yielding damper called Tapered Strip Dampers (TSD) for the purpose of retrofitting of damaged non-ductile RC frames. Their results showed that the stiffness degradation of the retrofitted RC frame was slower with better energy dissipation. Bruschi and Quaglini [16] introduced a novel hysteretic friction damper named prestressed lead damper with strait shaft (or PS-LED) and illustrated the damper efficacy for seismic retrofitting of out-dated RC frames, as compared to conventional steel hysteretic dampers.

This paper presents the experimental results obtained by the cyclic testing of a RC frame equipped with a self-centring friction damper named Resilient Slip friction Joint (RSFJ). The damper characteristics and performance behaviour has been investigated both in component and structural level [17]. Here, the damper is attached in a toggle bracing arrangement to the structure. Two identical one-story single bay RC frames were tested for this purpose (one serves as a benchmark bare frame while the second frame represents a retrofitted performance). The paper also covers the criteria considered for the design of the retrofit scheme in this research. While the design recommendations and outcomes presented here are based on a self-centring flag-shaped damper, it can also provide some information for retrofit designing with other dampers as well.

2. Toggle bracing systems

RSFJ is classified as a displacement-dependent device and thus, its performance depends on the relative displacement of its two ends. While many possibilities can be considered for connecting the joint to the

structure, the key locations are where the expected relative displacements are highest for the device. As for the non-seismically designed RC frame where the maximum permissible drift of the frame is limited (in the order of 1% or less), common installation of the joint such as diagonal and chevron may not provide considerable stiffness and relative displacement for the joint to dissipate the seismic energy. To tackle this issue, Toggle-bracing arrangement can be employed to amplify the small deflection of the frame into a large relative motion for the joint. The concept was introduced by Constantinou et al. [18] on viscous dampers and its effectiveness was verified through shaking table tests [19]. Fig. 1 depicts the common different arrangements of toggle bracing systems introduced by previous studies, in comparison to the diagonal and chevron bracing system. While the amplification factor (f) for each system is provided in Table 1. The following relationships exist for the installation of the joint in the toggle-bracing system:

$$u_d = f \times u \quad (1)$$

$$F = f \times F_d \quad (2)$$

Where u_d and F_d are the relative displacement and force along the axis of the joint, respectively. The parameters u and F denote the story displacement and horizontal component of the force exerted to the frame. The derivation of magnification factor for different arrangements of braces can be determined by considering a small deflection of the frame toward either left or right direction and assuming that all of the braces' deformations are focused in the dampers (i.e. the braces axial flexibility are neglected). Although the provided equations are useful for initial estimation of the damper deflection, the software modelling can estimate the damper deflection more accurately, as they can take into account the brace axial flexibility as well. Moreover, for the arrangements outside of the cases shown in the Fig. 1, the numerical software modelling is needed to compute the damper deflection against certain amount of frame drift.

Among the available arrangements, the lower toggle (Type II) (Fig. 1-f) was adopted here for the experimental testing, where the toggle brace system is connected to the three beam-column joints of the frame. It should be noted that the braces are assumed to be pin-connected to the beam-column joints and the designed connections can fully transfer the brace forces to the RC frame.

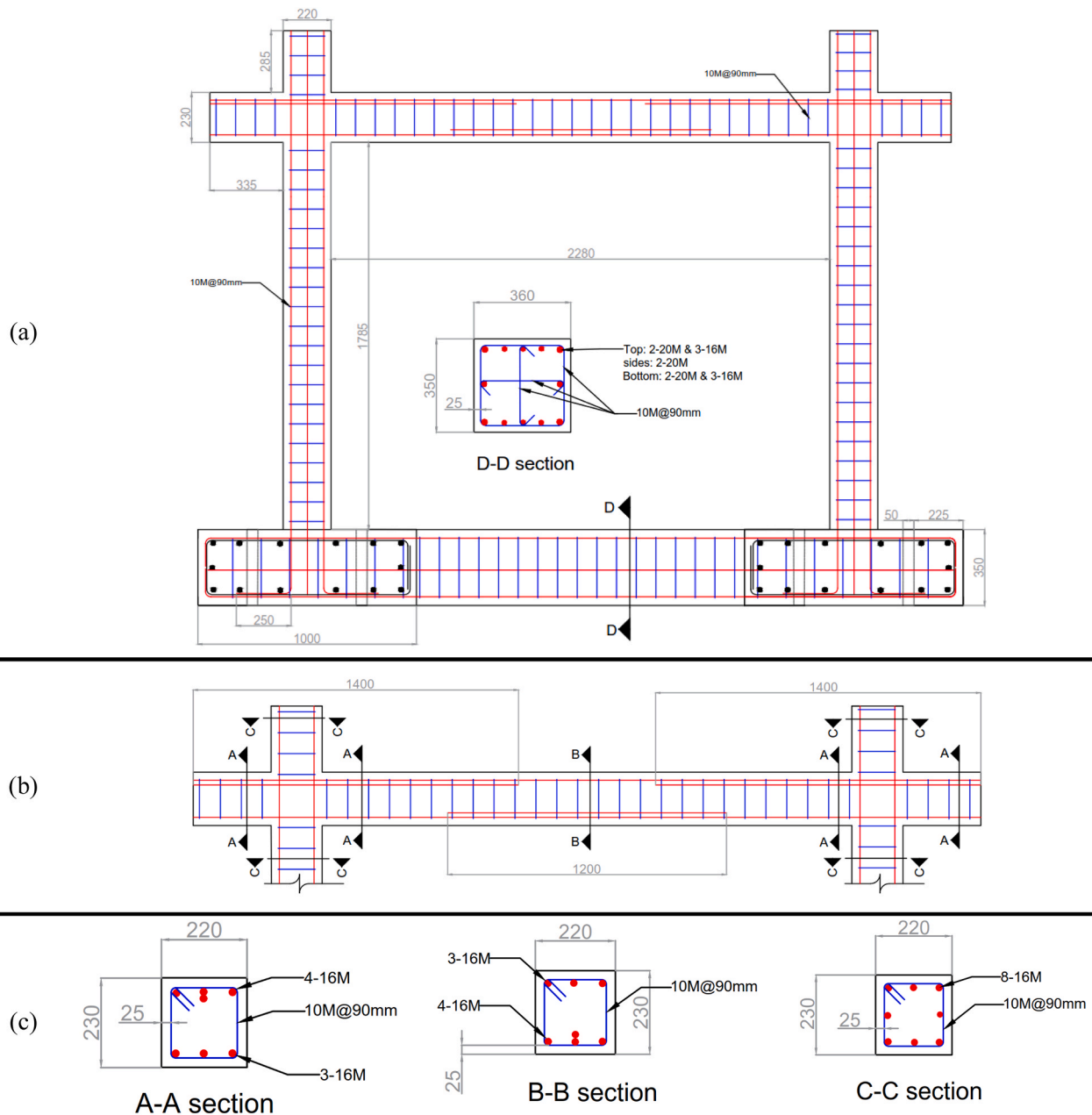


Fig. 2. The RC frame rebar detailing and section geometry dimension: (a) Overall height and length of the frame, and (b) to (c) frame beam and column section.

3. Deficient RC frame considerations

To check the efficacy of the RSFJ-toggle bracing system, two identical RC frame were manufactured for the experimental testing. The frames are similar to the RC frame studied by Al-Sadoon et al. [20,21], with scale factor of 0.6 and slight changes in dimension given the testing space limitations and bolt hole patterns in the strong-floor of the AUT University Structures lab. The frame specimens represent a good constructed pre-1970s gravity-only RC moment resisting frame with no specific seismic provisions. The bar details and dimensions of the frame are depicted in Fig. 2.

A few aspects were considered for the construction of these frames so they better represent an old-fashioned deficient RC frame. It is a possibility that old-fashioned RC frames were constructed with material and rebars that may not demonstrate the quality and characteristics of today's material and their characteristics are subject to change over time. For the retrofit purposes, the probable characteristics of materials

should be considered for analysis. Here, a low value for compressive strength of the concrete was considered (approximately 20 MPa) to better demonstrate a frame with low strength concrete. The compressive strength was then checked by concrete cylinder test.

Another critical aspect for the detailing of RC members, especially the columns is the amount of transverse reinforcing provided and in particular the spacing between the adjacent rebars. The transverse rebars provide confinement for the core concrete and prevent the buckling of longitudinal bars. The performance of non-ductile concrete RC members with light shear reinforcements have been extensively investigated in the literature [22,23]. In general, the lower shear reinforcement results in smaller drift capacity for such columns. Based on Engineering assessment guidelines (C5) [24], unconfined condition is present if at least one of the following conditions are exist in the RC frame:

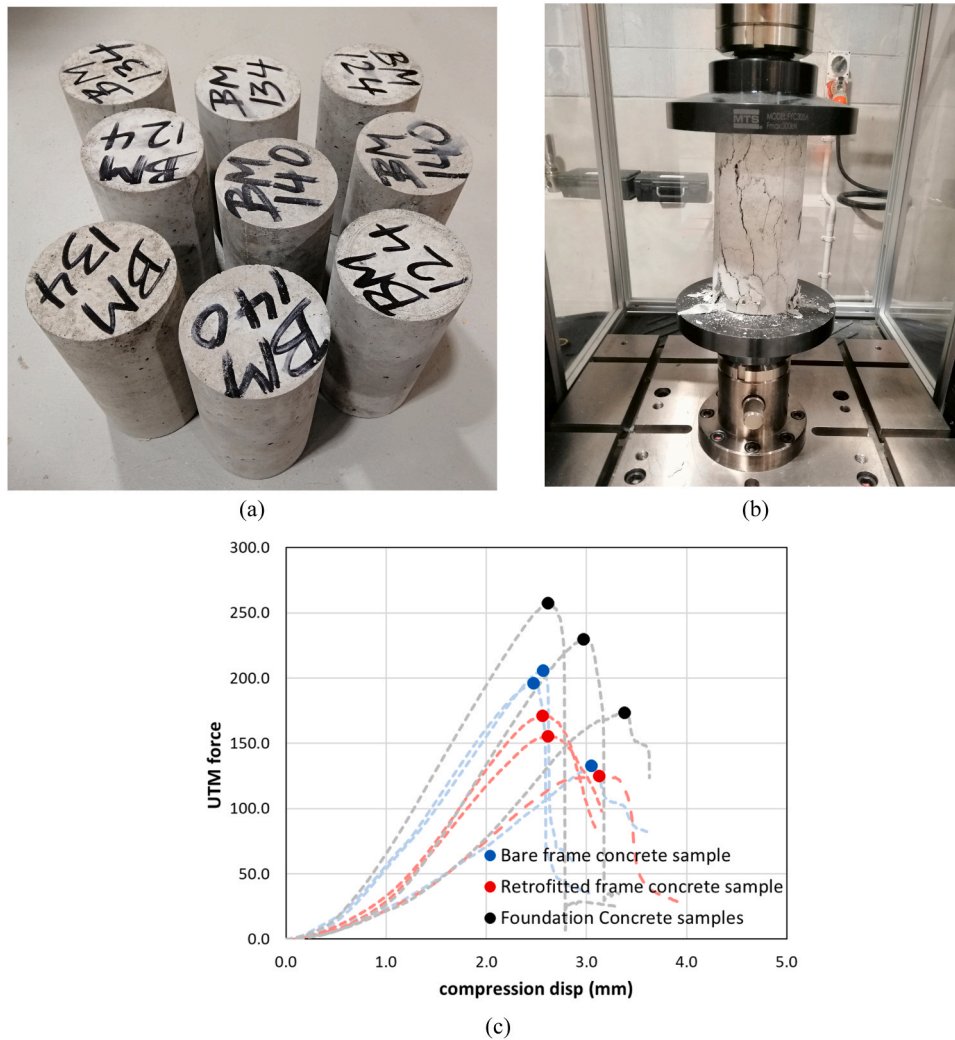


Fig. 4. Concrete cylinder testing of the frame: (a) nine samples for the frames and foundation, (b) testing the samples using UTM, (c) Obtained results.

If the friction in the pins is neglected, the braces will act in pure axial force and are in equilibrium at the point A. Thus, they follow the Lami's Theorem which states that when three forces acting at a point are in equilibrium, each force is proportional to the sine of the angle between the other two forces:

$$\frac{F_{Top\ brace}}{\sin\alpha} = \frac{F_{Bottom\ brace}}{\sin\beta} = \frac{F_{damper}}{\sin\gamma} \quad (12)$$

The top and bottom brace axial forces can be derived from above equation and needs to have sufficient capacity to withstand the damper ultimate force without any buckling or yielding. The buckling criteria of the braces will be explained in the next part. For the very short distance L ($\gamma \approx 180$), the small damper force would result in high top and bottom brace forces and thus uneconomical bigger sections for these two elements, while the bigger distance L would lead to smaller forces in the braces and might not justify using the toggle-bracing arrangement. For the current test setup ($\gamma = 154$, $\beta = 115$, $\alpha = 92$), the ultimate force of the damper-brace assembly was set to 48.8 kN, thus the top and bottom braces need to be designed for 111.25 kN and 100.9 kN, respectively.

6.2. Stability criteria

For a proper energy dissipation in the proposed bracing system, any possible buckling modes that may interrupt the performance of the braces need to be avoided. It has been shown that the compression

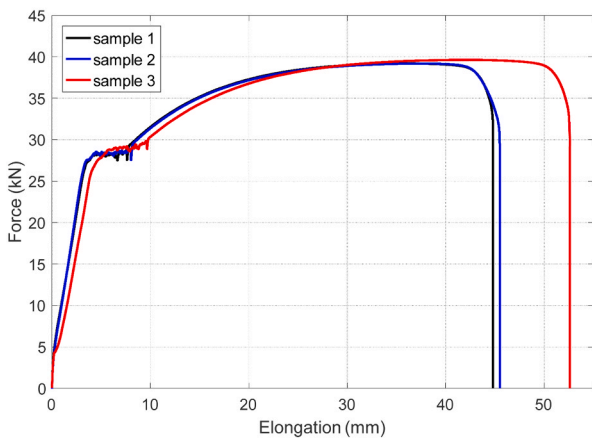
strength of the RSFJ might drop due to its rotation flexibility [26]. Therefore, an Anti-Buckling Tube (ABT) is added to the damper-brace assembly to present a symmetric hysteresis behaviour, both in tension and compression. It is worth noting that the stability analysis of the RSFJ is based on the assumption that the brace has an effective length factor of $K=1$ (i.e. the brace is pin-pin connected at both ends). Contrary to regular braces where the brace is pin-connected to rigid ends, the braces in toggle bracing system (including RSFJ damper-brace) are connected to one rigid end and one restrained end as can be seen in Fig. 10.

An optimised design for the system needs to assume the sections of the braces and end support characteristics, and then calculate the buckling load for each brace and make sure that the ultimate compressive strength of the RSFJ-brace is less than the buckling load capacity of the other two braces. The thorough buckling analysis of the RSFJ-toggle bracing system may require further analysis and is out of the scope of this paper. here, a conservative approach was taken to size the brace sections based on the effective length factor concept.

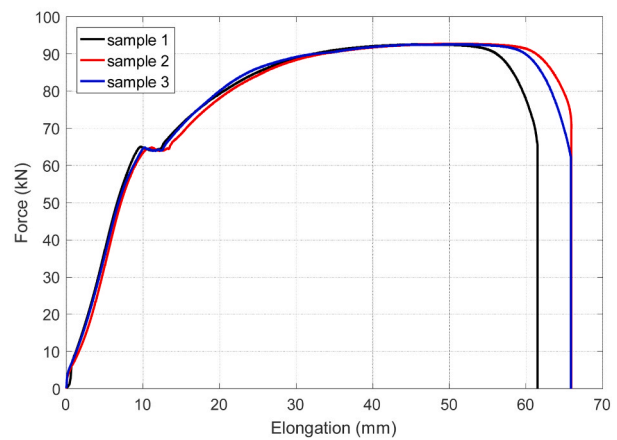
As can be noted from Fig. 10, the braces can be assumed to be pin-pin connected for the in-plane behaviour and connected as fixed-free for the out-of-plane behaviour. The presence of the pin at the point A and the five cleats that are connected to this point and designed to remain elastic would make the rotation of point A negligible. However, for the sake of simplicity and having a margin of safety, the influence of node A rotational and translational stiffness was disregarded for the AB and AC braces, while considering a large rotational stiffness for the point B and



(a)



(b)



(c)

Fig. 5. The tensile strength testing of the reinforcements employed in the RC frame: (a) testing the rebars using UTM, (b) results of M10 rebars, and (c) results of M16 rebars.

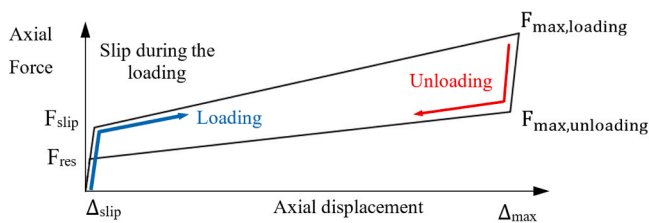


Fig. 6. RSFJ flag shape force-deformation relationship.

C (R_{kb} and R_{kc}). Therefore, both braces can be designed based on effective length factor $K=2.0$.

For the RSFJ-brace design, it can be stated that the effective length factor lies between an idealised pin-pin connection and the one with slight out-of-plane movement due to elastic out-of-plane movement of point A. Again, an effective length factor of 2 was considered for the

RSFJ-brace (thus neglecting the present restraints in the middle point), to provide a margin of safety for the damper-brace assembly. It should be noted that in case of out-of-plane bending of the brace, it is unlikely that the damper experiences any damage and it would only decrease its deflection capacity (thanks to the out-of-plane flexibility of the RSFJ).

The final check regarding the stability of the toggle-bracing system is the buckling analysis of the damper-brace assembly itself. On this basis, the damper-brace needs to be checked against two criteria that might limit the ultimate compression capacity of the damper-brace (Fig. 11):

- The stiffness deterioration path (the effects of $P-\delta$ and initial imperfection which inclines toward Euler buckling load as the lateral deformation increases). Such failure results in elastic buckling of the member rather than pure axial movement in the damper.
- The strength deterioration path which provides the axial strength of the system when a plastic hinge develops in the brace body or the ABT. Such failure usually ends up in a plastic hinge development in the brace.

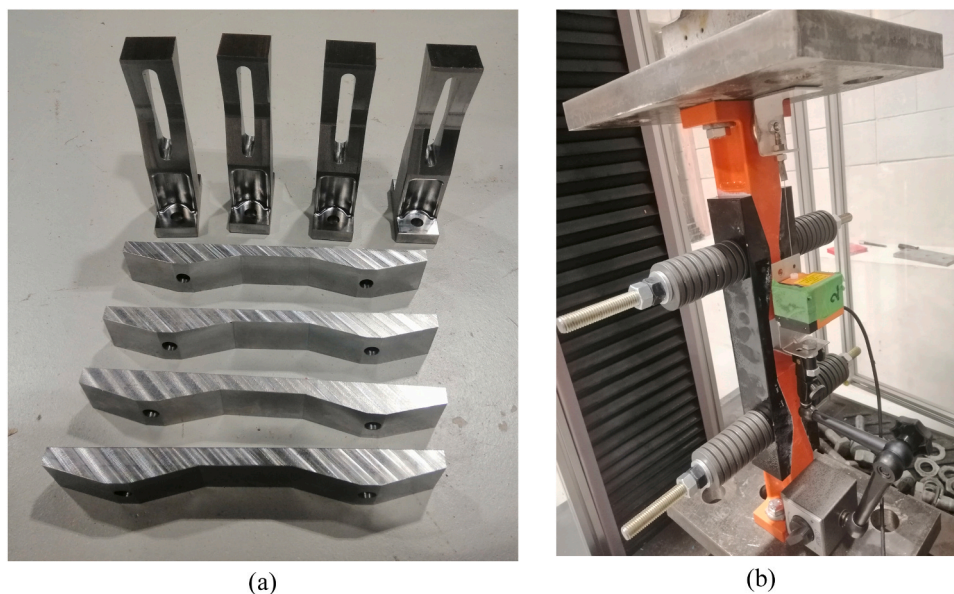


Fig. 7. RSFJ dampers component test: (a) Cap and middle slotted plates, (b) Assembly test setup.

Table 2

Tuning characteristics of the RSFJs for the experimental testing.

Parameter	Unit	Tuning scenario 1	Tuning Scenario 2
Disk Spring deflection capacity	mm	0.65	0.65
Slipping force (F_{slip})	kN	12.2	18.3
Ultimate force (F_{ult})	kN	24.4	24.4
Restoring force (F_{rest})	kN	6.3	6.3
Restored force (F_{resid})	kN	3.2	4.8
Joint max deflection (Δ_{ult})	mm	46.1	40.0
Prestressing force	kN	14	21
Prestressing ratio	%	50%	75%
No. of disk spring per side	-	19	33

The results of stability checking for damper-brace assembly are shown in Fig. 12. As can be seen, the force demand is below the Euler path and strength path which means the damper-brace would remain completely elastic during the test.

6.3. Frame restraints and connection design

Similar to the previous studies regarding RC frame retrofitting with braces [27], two main methods for connecting the RSFJ-toggle bracing system to the RC frame can be considered, namely the direct connection and indirect connection. Regarding the indirect connection, the retrofit braces can be assembled as a separate frame and attached to the side face of the RC-frame via post-installed anchors. Such a configuration may seem more expensive, it can be separately designed and then connected to the frame, collect the RC frame force in a more distributed manner and enable using larger brace sections and dampers. Other options would be to install the toggle-bracing system directly to the RC-frame, where the RC frame is connected to the braces at discrete locations (beam-column joints for this case). The efficiency of such system depends on the ability of the connection between RC frame and bracing member to successfully transfer the load. For the current test setup, the direct method has been implemented for the attachment of brace to the RC frame. On this basis, three distinct connection points were considered for the toggle-bracing system (Damper-brace connection, top brace connection and bottom brace connection).

As for the lateral restraints of the test setup, four adjustable timber blocks connected to a small I-section were employed to maintain the frame against out-of-plane movement (Fig. 13-a,b). The surface between

timber blocks and RC beam was lubricated to minimise the friction force contribution from the lateral restraints to the frame test results. Also, two shear keys that were available in the lab were employed in front and back of the frame to prevent the frame sliding during the cyclic loading (Fig. 13-c).

Fig. 14 shows the criteria considered for the design of gusset plate to fully transfer the braces axial forces to the RC frame. The pinned connection for the braces minimises the in-plane induced moment to the gusset plates. Regarding the design of the gusset plates for compression loads, it should be noted that unlike ordinary braced frames (where braces are expected to buckle for energy dissipation and gusset plates are designed for allowing this out-of-plane rotation), the RSFJ-Toggle bracing system dissipates the energy through damper component sliding. Therefore, the gusset plate should keep the braces in-plane during seismic loading. A number of methods have been introduced and explained by researchers to minimise the gusset plate out-of-plane buckling, such as using stiffeners on the gusset plate edges or using effective length factor of 2.0 for designing the gusset plates [28]. Here, a compression member with the length demonstrated in Fig. 14-e was considered for the gusset plate compression that is fixed-free and has a cross section equal to gusset plate thickness and pin diameter. Such a conservative assumption will ensure the elastic performance of the gusset plate against any possible out-of-plane bending with minimal displacement.

As for the connecting plates, they can be attached to the RC beam-column joint by either anchor bolts embedded within the RC member or using stud-bars which tie the connecting plates on both sides of the beams and columns. Obviously, the second method may be more suited for retrofitting plans and thus adopted here. As highlighted by Maheri and Yazdani [29], a linear varying normal component better represents the normal components forces in the connecting plate. The finite element (F.E.) modelling of the gusset plates verifies such distribution as well (Fig. 15). To develop the F.E. model of the gusset plates, the obtained brace forces from the damper ultimate force (Eq. (12)) were employed to apply the brace tensile force on the pin-hole surface of the gusset plate. It is worth noting that the ABAQUS software package [30] were used to perform the F.E. analyses and check the final design. A nonlinear Elasto-Plastic material ($E = 200$ GPa) with isotropic hardening was designated to the gussets plate with yielding stress and ultimate stress of 350 MPa and 480 MPa, respectively. The finite element analyses indicated that the stress value was within the material elastic

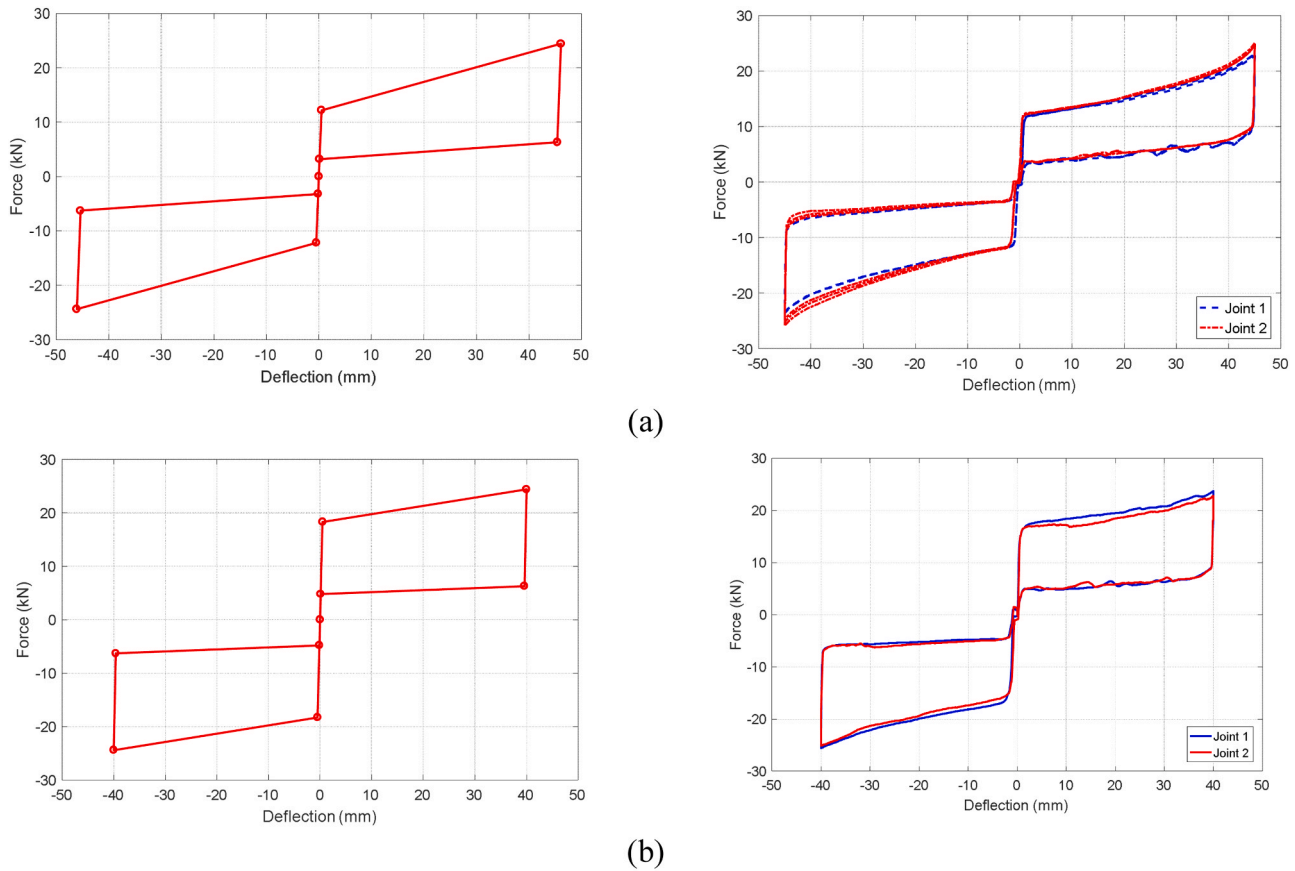


Fig. 8. RSFJ damper performance result: (a) calculated and observed hysteresis behaviour for the first tuning, (b) calculated and observed hysteresis behaviour for the second tuning.

range (less than 350 MPa). The model also highlighted that the stress values around the inner bolt holes were larger than the outer bolt holes.

Another concern regarding the gusset plate design was the risk of having undesired deformation of the gusset which is up-scaled in Fig. 15 for better clarity. On this basis, the connecting plates in the gusset plates might get bent and deformed during the tension force and jeopardise the system performance. Based on the finite element analysis of all three gusset plates, such deformation was less than 0.5 mm for all the gusset plates, thus the design seemed suitable for the test.

7. Experimental testing of the RC frames

In this section, the experimental testing results for the benchmark and the retrofitted frame are provided. The first frame (benchmark frame), was subjected to a progressive quasi-static cyclic pushover up to its failure (4.0% drift) to gain some insight about the performance of the frame without any retrofitting. Then, the second frame was retrofitted with the damper-brace system and went through the similar lateral loading up to 1.5% drift. It was decided to tune the damper with higher prestressing force and more disk springs, and repeat the test on the frame which already pushed up to 1.5% drift. Such a testing scenario could present the benefits of having an adjustable damper that can provide some level of flexibility for the designer. It can also demonstrate the performance of an already-damaged frame that receives retrofitting. It should be noted that all the frame tests were applied in quasi-static cyclic pushover manner.

7.1. Instrumentation and cyclic testing protocol

Fig. 16 presents the instrumentation layout used for the RC frame. A number of linear variable differential transformers (LVDTs) were placed

on each end of the beams, columns and foundation, to catch any displacement or sudden cracks during testing, while two calibrated draw-wires were employed to read the frame and damper displacements. A total vertical load of 440 kN was applied to the frame via six prestressed rods, whereas the lateral loading was exerted to the frame using a hydraulic actuator with the loading rate of 0.5 mm/s.

Fig. 17 shows the loading protocol for the benchmark bare frame up to 2.5% drift ($\Delta = 52.5$ mm). Each drift level was repeated for three cycles and at the third cycle, frame was held at the maximum of the pulling direction (towards right), so that visual damage occurred on the concrete surface be easier to spot. Moreover, the frame was painted with thin layer of white colour at the potential cracking zones.

Four distinct crack width (C_w) limits were assumed for the observing of the evolution of crack pattern in the RC frame [31] with each limit associated with a colour for marking on the frame:

- $C_w < 0.2$ mm: Representing narrow cracks on the surface (Green)
- $0.2 \text{ mm} \leq C_w < 1.0$ mm: Visible but narrow cracks (Blue)
- $1.0 \text{ mm} \leq C_w < 2.0$ mm: local crush of covered concrete (Red)
- $C_w \geq 2.0$ mm: Remarkable crush of concrete with cover spalled off (Black)

Fig. 18 presents the observed cracks in the RC frame during 0.5%, 1.0%, 1.5% and 2.0% lateral drifts. The cracks were measured using a metric feeler gauge. As can be seen, in 0.5% drift (Fig. 18-a), only narrow flexural cracks were witnessed at the top and bottom ends of the columns. As for the 1.0% drift (Fig. 18-b), the number and width of the cracks were increased. It should be noted that the presence of cracks in the columns were more evident than in the beam. As for the 1.5% drift, the first crack with $C_w \geq 1.0$ mm was witnessed at the top and bottom of

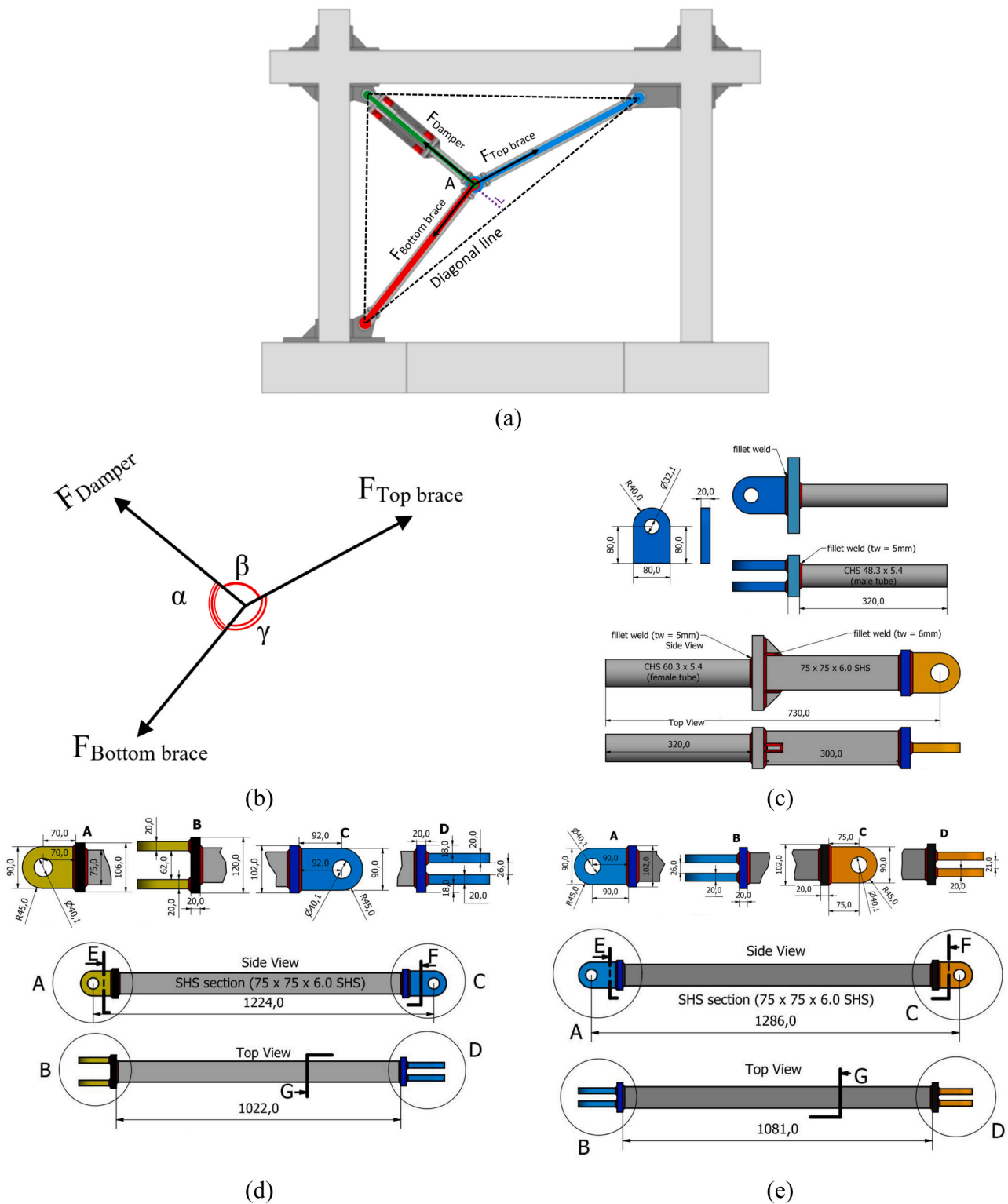


Fig. 9. Parameter definition of the toggle-bracing forces and the brace sections.

the RC frame column, with some diagonal visible narrow cracks in the beam column joint area. Regarding the observed damage in 2.0% drift, the concrete crush with crack width larger than 2.0 mm was witnessed at both columns, along with large flexural cracks ($C_w \geq 2.0$ mm) on the beam as well.

In general, the failure mode of the frame was the formation of flexural cracks at the end of columns. Based on the observed cracks patterns, it seemed reasonable to assume that the retrofitted frame would start to

accumulate noticeable damage if the drift reaches to 1.5%. Albeit, no local crush of concrete ($C_w \geq 1.0$ mm) was observed on the retrofitted RC frame (It needs to be stated that due to presence of stud bars and connection plates at the corners of the retrofitted RC frame, it was difficult to witness and mark the cracks on the retrofitted frame). This may be due to the fact that the connection could have a confinement effect on the beam-column joints and better distribute the crack over the length of the structural member, while in the bare frame, the cracks were

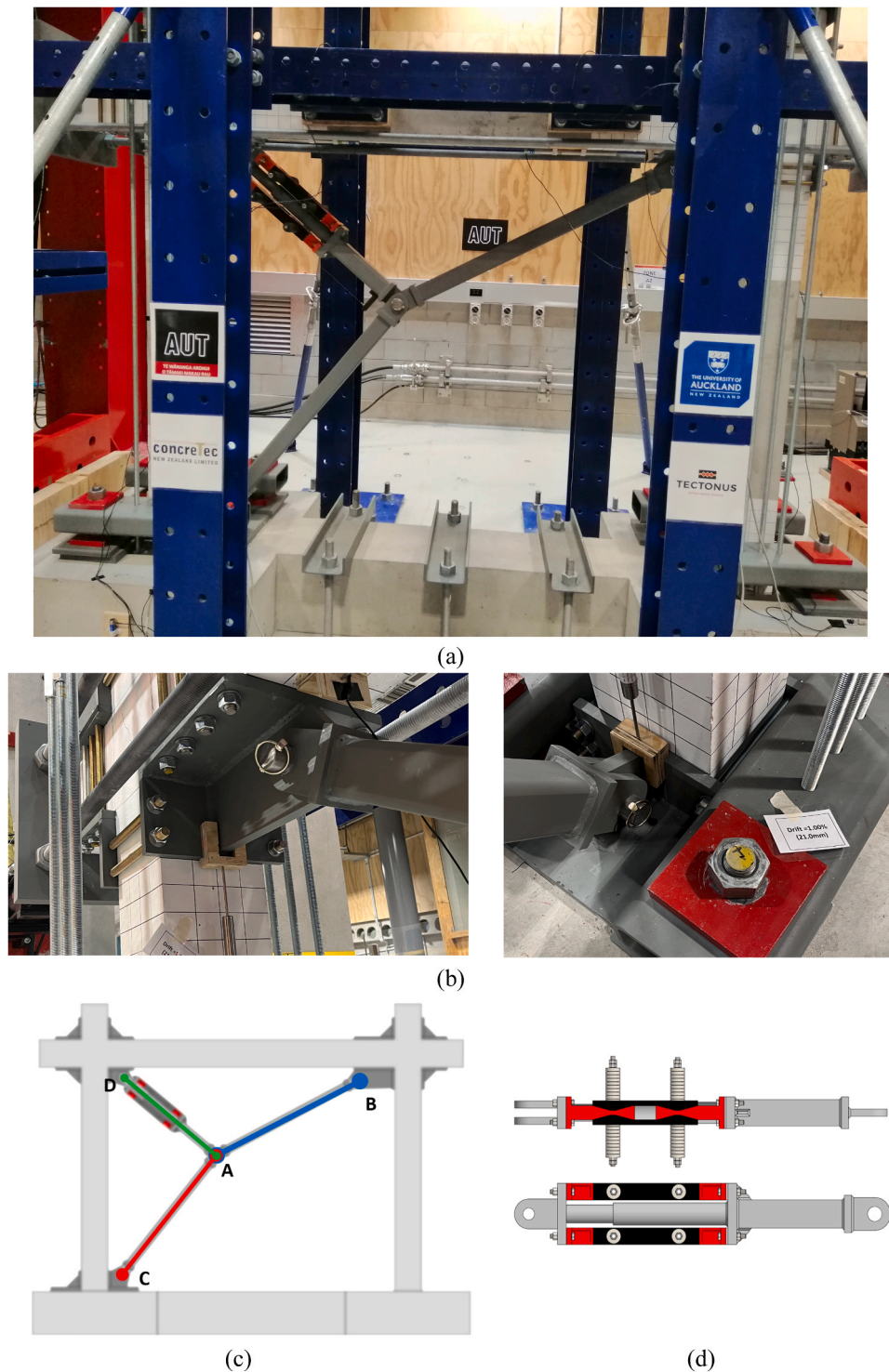


Fig. 10. The RC RSFJ-toggle bracing test setup: (a)The overall view of the test-setup, (b) the pinned connections for the braces, (c) constraint naming for the test setup; and (d) the RSFJ damper-brace assembly.

mostly concentrated at the beam and columns ends.

7.2. Discussion of the gravity loading accuracy

By taking a look at the literature, different methods have been employed to impose the dead load on the RC structural frame, such as using heavy steel blocks, using actuators or hydraulic jacks, or using prestressed cables or rods. The third method was adopted here by designing an especial rod holding assembly on top of the columns to hold the rods;

then a total number of 12 *M18 high strength rods (6 rods for each column) were prestressed up to 36–37 kN (total loading of 220 kN per column). It is possible that during large lateral drifts of the RC frame, the axial capacity of the rods become engaged in the lateral load resisting of the structure due to “rope effect” and falsely contribute to the recorded base shear of the frame (Fig. 19). To investigate the rope effect on the experimental test, a donut load cell was attached to each of the three prestressed rods and captured the load during different drift values up to 3.0%. For safety reasons, interpolation values (polynomial

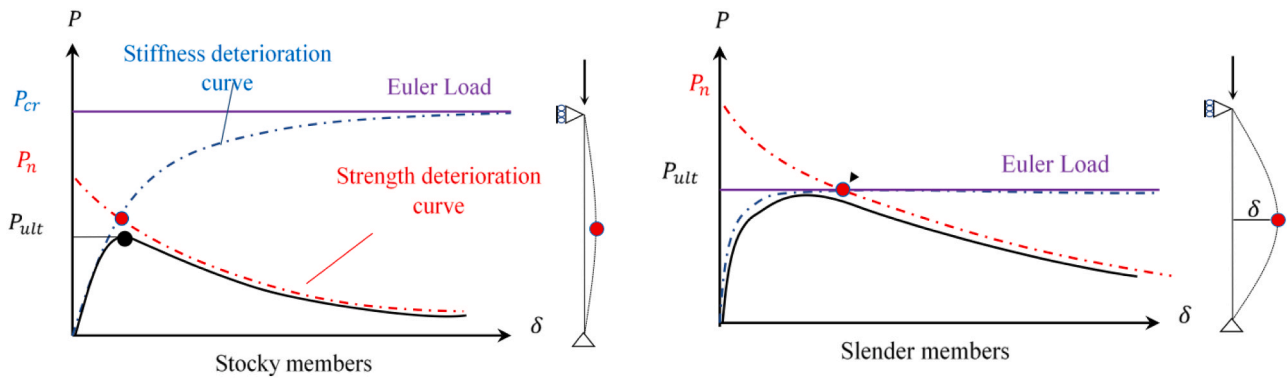


Fig. 11. Compressive performance of steel braces and their potential failure modes.

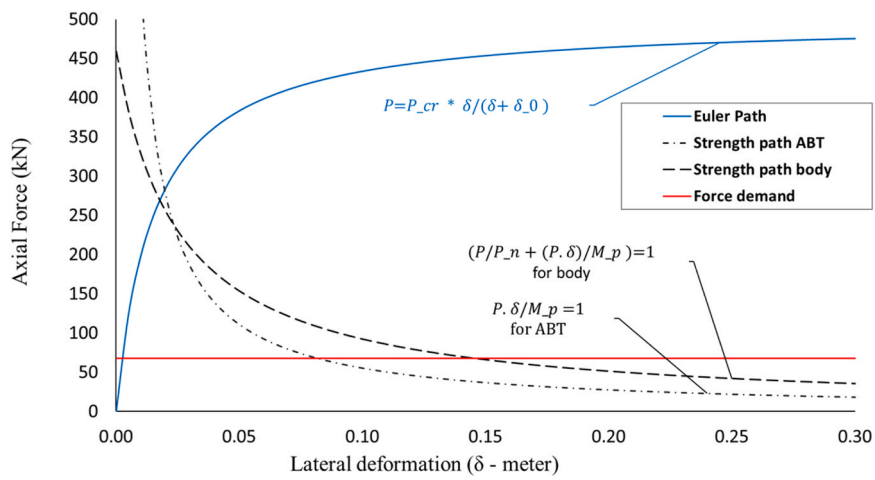


Fig. 12. Results obtained from the stability analysis of the Damper-brace assembly.

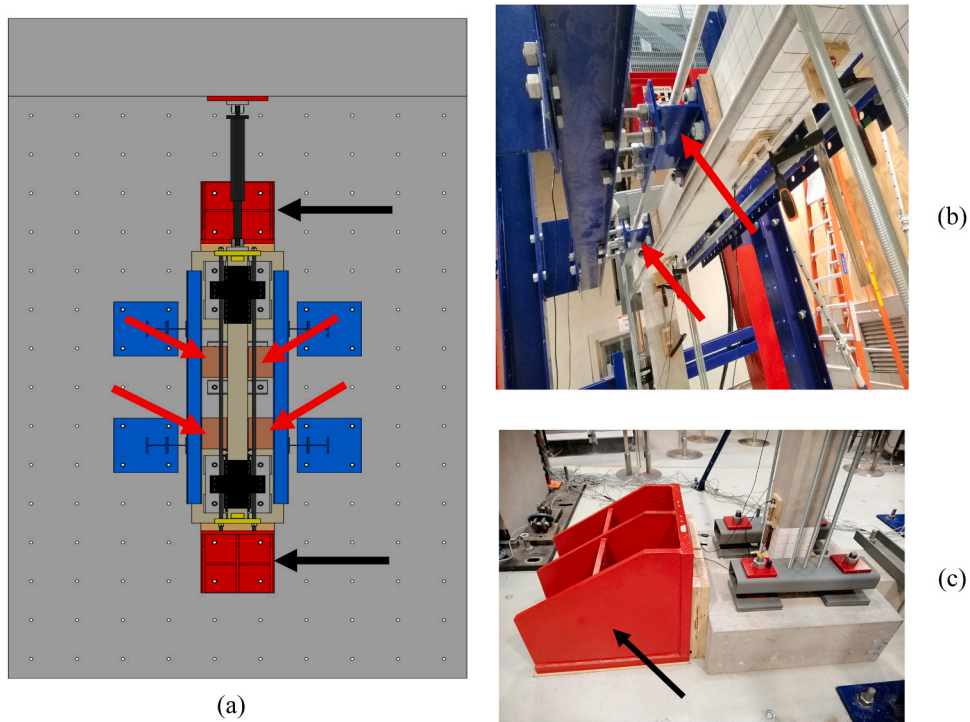


Fig. 13. RC Frame restraints: (a) top view, (b) lateral support provided for the RC frame (red arrow); and (c) shear key that prevents frame sliding (black arrow).

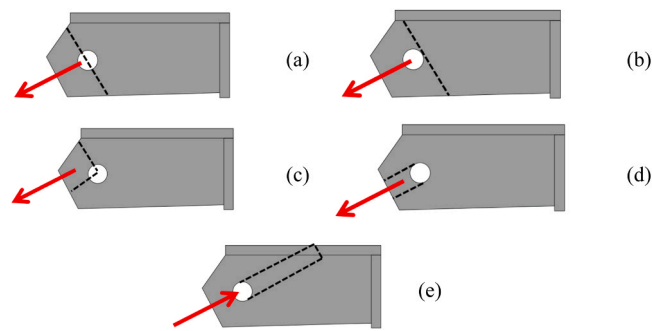


Fig. 14. Gusset plate design criteria: (a) net section fracture, (b) gross section yielding, (c) block shear combined with tension and (d) pure shear tear out (e) compression member for gusset plate design.

interpolation, order=2) were utilised for 4.0% drift, rather than performing the procedure.

Table 3 shows the changes in horizontal and vertical forces of prestressed rod during different drift levels. As can be seen from the table, the applied gravity loading remains unchanged for the small drift and almost no contribution to the base shear is expected from the rods. However, higher frame drifts would result in higher horizontal load contribution of the prestressed rods. Fig. 20 compares the new backbone curve for the bare frame and the retrofitted one. It should be stated that the new backbone curve was obtained by subtracting the rope effect contribution from the previous one. On this basis, the overall lateral force contribution from the rods is evaluated as around 7.0 kN at 1.5% drift.

7.3. Results and discussion

In this section the obtained results from the RC frames are provided. Three distinct testing were conducted on the frames which is listed below:

- Benchmark bare frame (the first RC frame): While the bare frame was tested up to 4.0% drift, only the result up to 1.5% drift is provided, for better comparison with the retrofitted cases.
- Retrofitted frame (the second RC frame-intact), Test 1: The second frame was equipped with the toggle-bracing assembly and the dampers were tuned as per first tuning scenario in Table 2 ($F_{\text{slip}}=12.2$ kN, $\Delta_{\text{max}}=46.1$ mm).
- Retrofitted frame, Test 2: Since the second frame that was already pushed up to 1.5% drift, remained in a good condition with crack width smaller than 1 mm, it was decided to increase the prestressing force of the damper and the number of disk springs as per second tuning scenario in Table 2 ($F_{\text{slip}}=18.3$ kN, $\Delta_{\text{max}}=40.0$ mm) and redo the cyclic testing on the second frame.

Fig. 21 presents the lateral load response versus the lateral deformation of the bare frame up to 1.5% drift. The hysteresis behaviour reveals the gradual decrease of lateral stiffness during the elastic range of loading, due to cracking of the concrete, however the behaviour becomes stable in the third cycle. Moreover, the numerical pushover simulation with SAP2000 [32] is presented as well. Fibre hinges were employed for the member nonlinearity and the materials were calibrated with the concrete cylinder tests and rebar tensile test results, to reduce the uncertainty between numerical and experimental results. The ultimate strength for the pull and push directions were recorded as 112 kN and 100 kN respectively, while the SAP2000 gives approximately the same results (96.8 kN). The small difference between the numerical and the experimental results could be due to the contribution of prestressed rods and minor friction between lateral restraints and the RC frame.

As for the test 1 (intact frame with damper $F_{\text{slip}}=12.2$ kN, depicted

in Fig. 22), the experimental results highlight the improved performance of the frame, in terms of energy dissipation, increased stiffness and self-centring behaviour. The pinching behaviour of the bare frame was replaced with semi-flag shape behaviour. The ultimate strength of the retrofitted system is recorded as 172 kN and 162 kN. Some levels of stiffness and strength degradation is witnessed in the retrofitted frame, due to concrete cracking and accumulated frame damage. Moreover, the presence of connection plates embracing the beam-column joint have helped towards distribution of concrete crack over larger area of beam and columns. Based on the performance of the toggle-bracing, the braces performed as expected without any instability issues and out-of-plane movement of the restrained node. While for this current test, the retrofitted frame showed negligible residual drifts, it is possible for the frame to present some residual displacements in higher drift demand. This indeed depends on the target level of drift for the frame, as well as the restoring force provided by the joints in the system.

The damper displacement during the cyclic loading is summarised in Table 4. Based on the test results, the amplification factor in the pull and push directions of the system is evaluated as 1.16 and 0.98, respectively. The damper displacement from numerical results also provides very close results. The results shown in the table also highlights the capability of the proposed system to be activated within a small drift of the RC frame. As an illustration, for the 0.25% drift of the RC frame (5 mm frame lateral deformation), the damper has already mobilised more than 2 mm.

The numerical outcomes for a cyclic pushover with 1.0% and 1.5% drifts are compared with the experimental results in Fig. 23. While the numerical results are generally in good agreement with the experimental data, some level of difference is witnessed, especially in residual displacement results, which is slightly higher in the numerical outcomes for the 1.5% drift. This is due to the difference in true nonlinear behaviour of the frame, against the simplified mathematical model that may not consider all the aspects of RC frame. Such difference is not witnessed for the 1.0% drift case given the system is mainly behaving elastic in this drift ratio.

After finishing the cyclic test on the retrofitted frame, the dampers were tuned with higher prestressing force and more disk springs (shown in Fig. 8-b). The second retrofit test could represent the inclusion of retrofit for the frames that already experienced some level of earthquake damage (up to 1.5% drift in this case). It should be pinpointed though, that the damage level is not critical, otherwise it might be necessary to repair the frame, then attach the retrofitting braces. The experimental data for the second retrofit testing is compared with the first test in Fig. 24. For the second test, the RC frame has already experienced some concrete cracking when pushed up to 1.5% drift, thus no stiffness degradation was seen in the hysteresis behaviour of the second test. This also verifies the resilient and repeatable behaviour of the retrofit solution over the three cycles of testing. The ultimate strength of the frame for the second test was recorded as 164 kN and 192 kN for the push and pull directions, respectively. The damper displacements during the

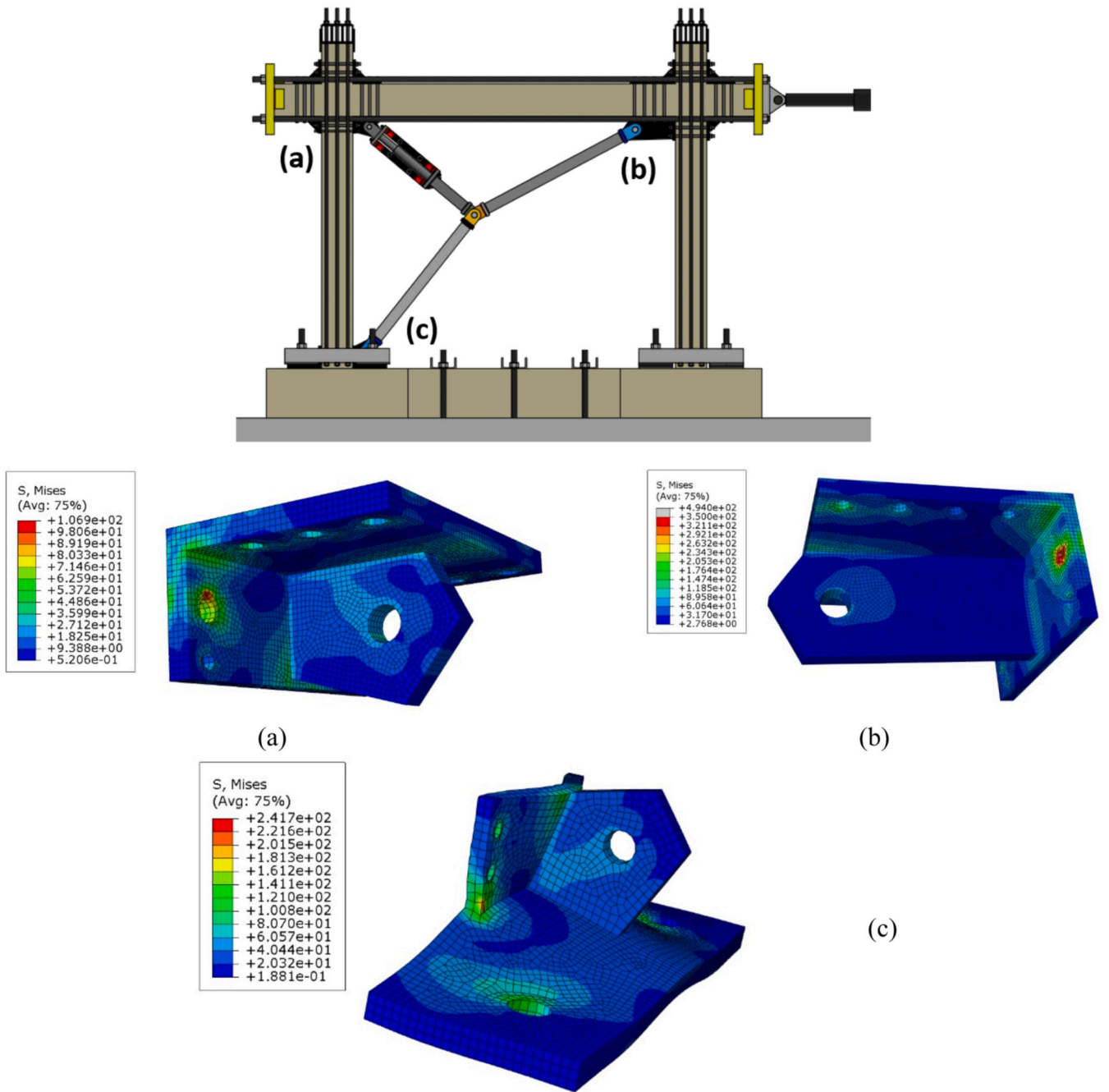


Fig. 15. FE analysis of gusset plate: (a) damper brace, (b) top brace, and (c) bottom brace.

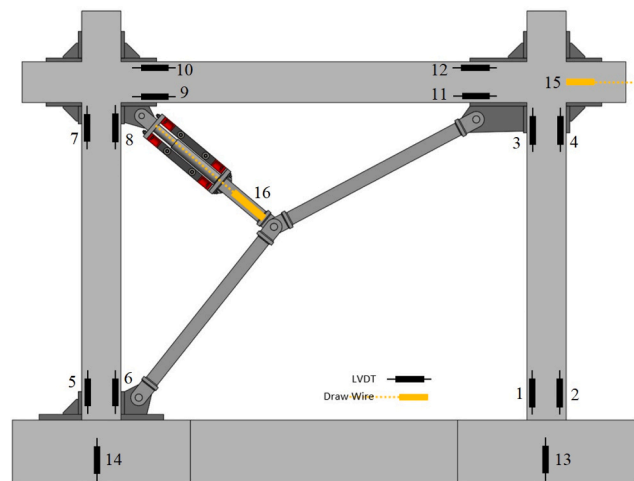


Fig. 16. Instrumentation layout.

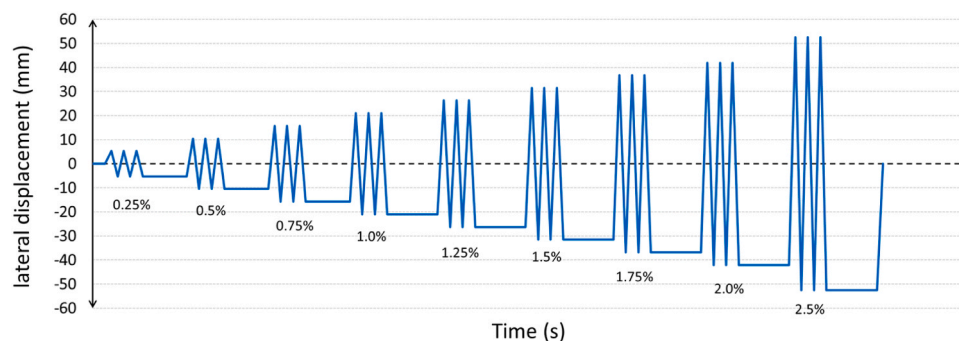


Fig. 17. Lateral loading history of the benchmark frame.

second retrofit test were the same as the first test.

The absolute energy dissipation (i.e., the area enclosed by the hysteresis curve of the RC frame) for the bare frame and the retrofitted cases are provided in Fig. 25. As can be seen, energy dissipation capability for the second retrofit is slightly higher than the first retrofit, noting that the energy dissipation for the second test does not contain any concrete crushing or frame damage. Since the hysteretic damping ratio of the RSFJ dampers were increased for the new tuning scenario, more energy dissipation was granted to the retrofitted frame. By accumulating the dissipated energy for all the cycles, the first and second retrofitted cases dissipated 245% and 285% of the benchmark bare frame (16% more energy dissipation for the second retrofit test, as compared to the first retrofit test). While the prestressing increment would provide some level of flexibility for the engineers to modify their design, it would increase the number of required disk springs for the joints.

8. Summary and conclusion

This paper investigated the efficiency of the RSFJ-toggle bracing system. Two small-scale identical RC frames were constructed and subjected to a quasi-static cyclic loading and the results of the benchmark frame and the retrofitted frame were compared. The following conclusions and recommendations are drawn:

- The overall performance of the retrofitted frame improved in terms of stiffness, strength and energy dissipation features. The ultimate strength almost doubled and energy dissipation increased 285%. It needs to be pointed that such results are only applicable to the

current experimental test and may not be generalised to other RSFJ-toggle bracing systems.

- The proposed retrofitting system is capable of being activated in small drift values (0.25%) and preserves the RC frame.
- The retrofitted braces performed as predicted without any instability issues and out-of-plane buckling.
- The connection plates were able to preserve the RC frame from concentrated damage at the beam and column ends and provide some level of confinement for the beam-column joints. This was witnessed by lesser number of cracks on the retrofitted RC frame up to the 1.5% drift.
- It needs to be stated that such retrofit may impose higher base shear on the foundation of the system. This needs to be considered by engineers for a proper retrofit design.
- The results and findings from this paper could be used for the design of the toggle-brace retrofitting of RC frames with other types of dampers such as traditional friction dampers. Obviously, such dampers may provide higher added damping to the retrofitted system. However, they might be more susceptible to residual drifts. A thorough comparison between self-centring and traditional friction dampers for retrofit purposes is planned for further research studies by authors.

Declaration of Competing Interest

On behalf of the authors, I, Sajad Veismoradi declare that we have no known competing financial interests or personal relationships that could have appeared to influence the work reported in this paper.

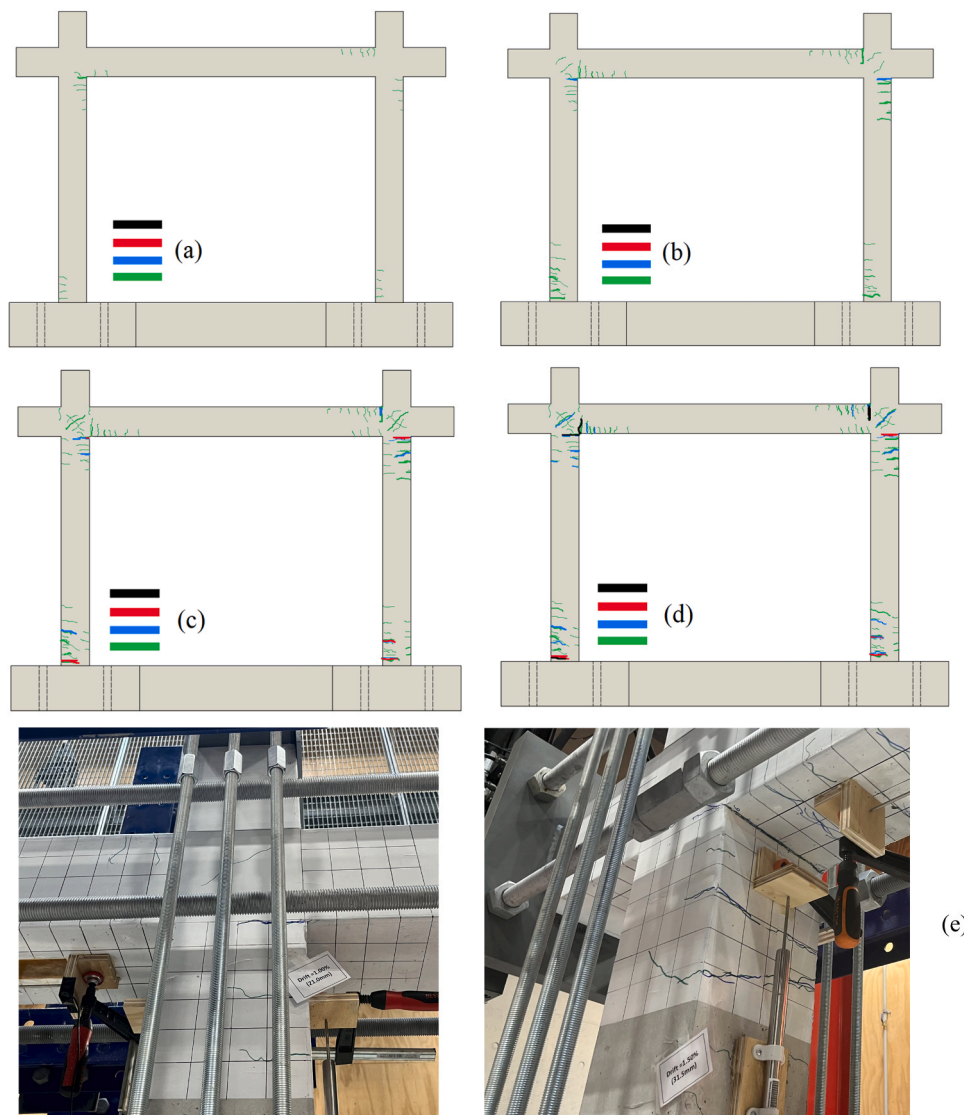


Fig. 18. Crack patterns of the bare frame in different drift levels: (a) 0.5%, (b) 1.0%, (c) 1.5%, (d) 2.0%, and (e) Sample photo of physical damages (cracks) on the benchmark frame.

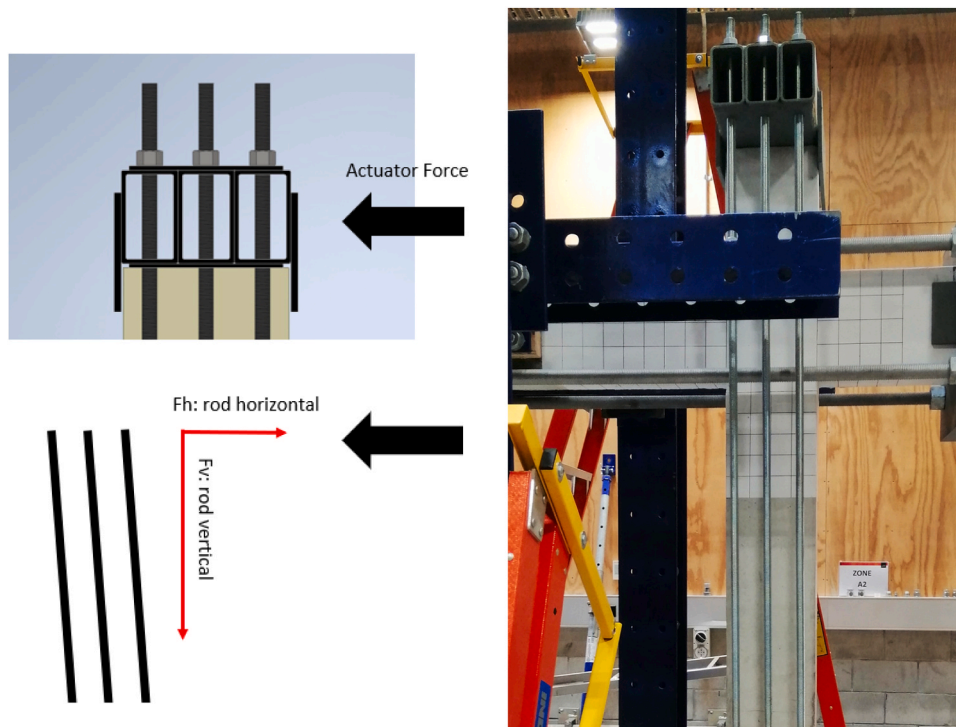


Fig. 19. The rope effect contribution on the recorded base shear of the frame.

Table 3
Changes in the rods prestressing forces due to drift.

Parameter	Unit	Drift values						
		0.0	0.5	1.0	2.0	2.5	3.0	4.0
$F_{\text{left rod}}$	kN	36.1	34.8	34.0	33.4	33.8	34.8	-
$F_{\text{middle rod (kN)}}$	kN	36.1	36.2	36.8	39.6	41.2	44.0	-
$F_{\text{right rod (kN)}}$	kN	36.4	37.7	40.4	46.5	50.6	55.0	-
$F_v = F_{\text{rod, total (kN)}}$	kN	217.2	217.3	222.4	239.0	251.2	267.5	306.7
changes in $F_{\text{rod, total}}$ (%)	%	0.0	0.1	2.4	10.0	15.7	23.2	41.2
$F_{h, \text{ total}} = 2 * F_h$	kN	0.0	2.2	4.4	9.6	12.6	16.1	24.5

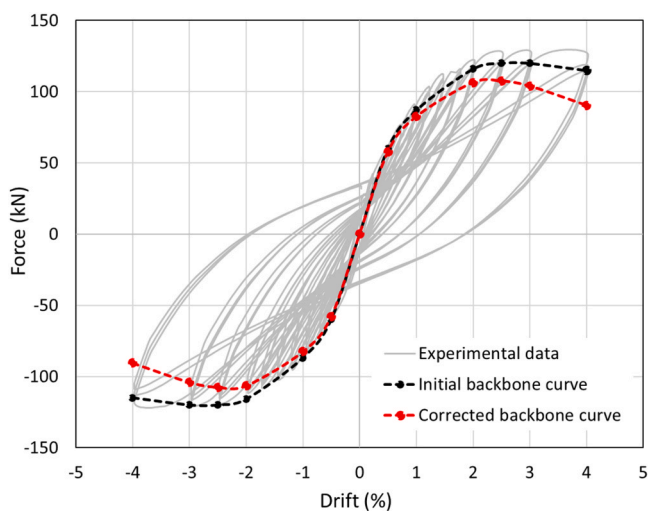


Fig. 20. Comparison of the initial and corrected backbone curve for the benchmark RC frame.

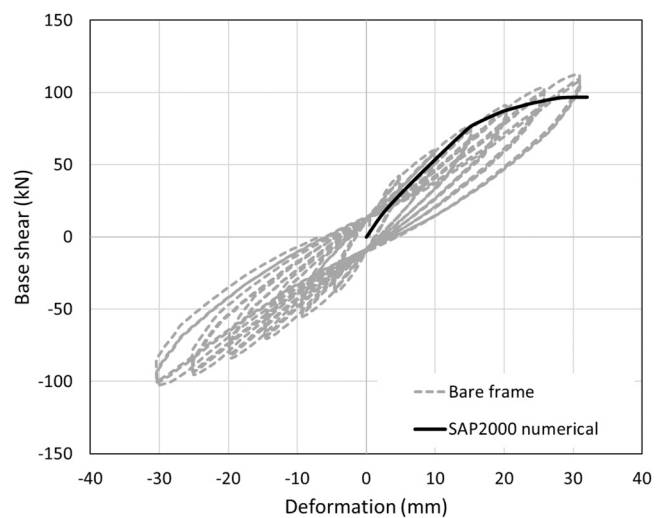


Fig. 21. Hysteretic lateral load-lateral deformation of the bare frame up to 1.5% drift.

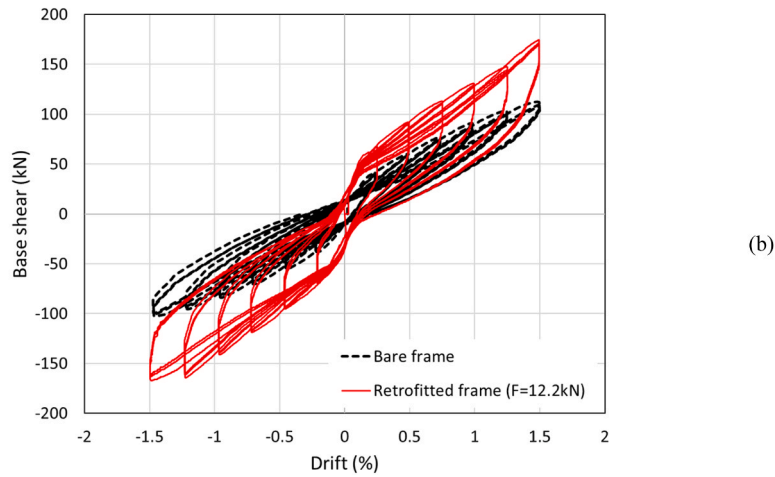


Fig. 22. Retrofitted frame performance: (a) Sample photos of RSFJ damper in the frame (b) Cyclic performance comparison of retrofitted frame against the benchmark frame.

Table 4
Recorded damper displacement during cyclic testing.

Parameters	Unit	Frame Drift (%)						
		0.25	0.50	0.75	1.00	1.25	1.50	
Frame displacement	mm	±5.3	±10.5	±15.8	±21.0	±26.2	±31.5	
damper displacement (pull)	mm	+3.2	+9.3	+16.3	+22.1	+29.1	+36.6	
damper displacement (push)	mm	-2.4	-7.5	-13.0	-18.3	-23.6	-30.7	

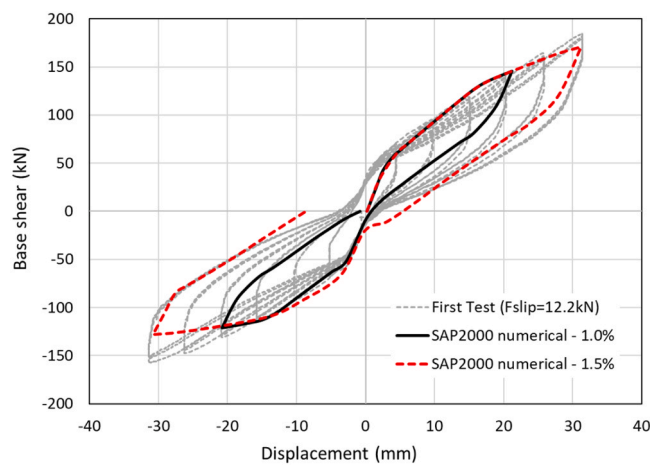


Fig. 23. Numerical model results of the retrofitted frame.

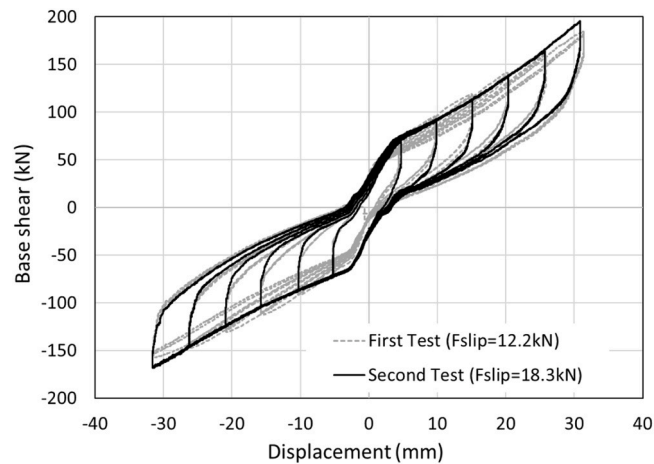


Fig. 24. Experimental results for the second retrofit test vs. the first retrofit test.

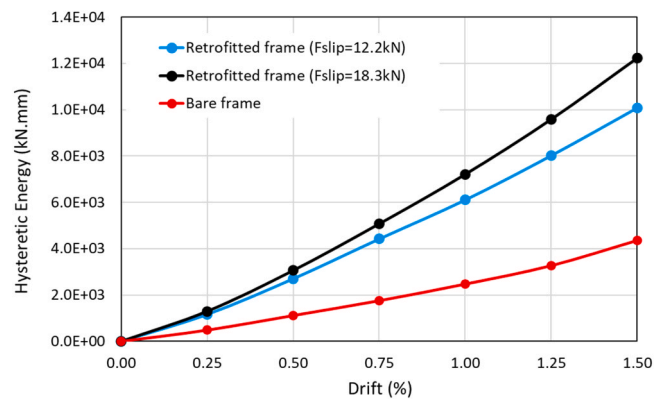


Fig. 25. Energy dissipation comparison for each drift ratio.

Acknowledgement

The authors appreciate the Ministry of Business, Innovation and Employment (MBIE) of New Zealand for the financial support of this study.

References

- O'Reilly GJ, Sullivan TJ, Monteiro R. On the seismic assessment and retrofit of infilled RC frame structures; 2018.
- Joseph R, Mwafy A, Alam MS. Seismic performance upgrade of substandard RC buildings with different structural systems using advanced retrofit techniques. *J Build Eng* 2022;59:105155.
- Karayannis CG, Chaliouris CE, Sirkelis GM. Local retrofit of exterior RC beam-column joints using thin RC jackets—an experimental study. *Earthq Eng Struct Dyn* 2008;37(5):727–46.
- Santarsiero G, Masi A. Seismic performance of RC beam-column joints retrofitted with steel dissipation jackets. *Eng Struct* 2015;85:95–106.
- Veismoradi S, et al. Seismic strengthening of deficient RC frames using self-centering friction haunches. *Eng Struct* 2021;248:113261.
- Cao X-Y, et al. Seismic retrofitting of existing frame buildings through externally attached sub-structures: state of the art review and future perspectives. *J Build Eng* 2022;57:104904.
- Naeem A, et al. Development and experimental verification of self-centering disc slit damper for buildings. *J Constr Steel Res* 2023;201:107759.
- Javidan MM, Kim J. Seismic retrofit of soft-first-story structures using rotational friction dampers. *J Struct Eng* 2019;145(12):04019162.
- Javidan MM, Kim J. A rotational friction damper-brace for seismic design of resilient framed structures. *J Build Eng* 2022;51:104248.
- Javidan MM, Kim J. A ductile steel damper-brace for low-damage framed structures. *Steel Compos Struct* 2022;44(3):311–23.
- Javidan MM, Chun S, Kim J. Experimental study on steel hysteretic column dampers for seismic retrofit of structures. *Steel Compos Struct* 2021;40(4):495–509.
- Nasab MSE, et al. Experimental study on seismic retrofit of a RC frame using viscoelastic dampers. *Structures*. Elsevier; 2021.
- TahamouliRoudsari M, et al. Experimental assessment of retrofitting RC moment resisting frames with ADAS and TADAS yielding dampers. *Structures*. Elsevier; 2018.
- Di Sarno L, Manfredi G. Seismic retrofitting with buckling restrained braces: Application to an existing non-ductile RC framed building. *Soil Dyn Earthq Eng* 2010;30(11):1279–97.
- Vafaei M, Sheikh AMO, Alih SC. Experimental study on the efficiency of tapered strip dampers for the seismic retrofitting of damaged non-ductile RC frames. *Eng Struct* 2019;199:109601.
- Bruschi E, Quaglioni V. Assessment of a novel hysteretic friction damper for the seismic retrofit of reinforced concrete frame structures. *Structures*. Elsevier; 2022.
- Hashemi A, et al. Seismic resistant rocking coupled walls with innovative Resilient Slip Friction (RSF) joints. *J Constr Steel Res* 2017;129:215–26.
- Constantinou MC, et al. Toggle-brace-damper seismic energy dissipation systems. *J Struct Eng* 2001;127(2):105–12.
- Hwang J-S, Huang Y-N, Hung Y-H. Analytical and experimental study of toggle-brace-damper systems. *J Struct Eng* 2005;131(7):1035–43.
- Al-Sadoon Z. Seismic retrofitting of conventional reinforced concrete moment-resisting frames using buckling restrained braces. *Université d'Ottawa/University of Ottawa*; 2016.
- Al-Sadoon ZA, Saatcioglu M, Palermo D. New buckling-restrained brace for seismically deficient reinforced concrete frames. *J Struct Eng* 2020;146(6):04020082.
- Stirrat A, et al. Seismic performance assessment of non-ductile columns. In: *Proceedings of the 2014 NZSEE conference: New Zealand Society of Earthquake Engineering NZSEE*; 2014.
- Elwood KJ, Moehele JP. Drift capacity of reinforced concrete columns with light transverse reinforcement. *Earthq Spectra* 2005;21(1):71–89.
- Guideline N. Part C5, concrete buildings, technical guidelines for engineering assessments; 2017.
- Priestley M, Calvi G, Kowalsky M. *Direct displacement-based seismic design of structures*. NZSEE Conf 2007.

- [26] Yousef-beik SMM, et al. Effect of second-order actions on the performance of resilient slip friction joints: analytical and experimental investigation. *Structures*. Elsevier; 2021.
- [27] Pan KY, et al. Seismic retrofit of reinforced concrete frames using buckling-restrained braces with bearing block load transfer mechanism. *Earthq Eng Struct Dyn* 2016;45(14):2303–26.
- [28] Wu AC, et al. Hybrid experimental performance of a full-scale two-story buckling-restrained braced RC frame. *Earthq Eng Struct Dyn* 2017;46(8):1223–44.
- [29] Maheri MR, Yazdani S. Design of steel brace connection to an RC frame using Uniform Force Method. *J Constr Steel Res* 2016;116:131–40.
- [30] Systèmes D. Abaqus 6.14—Abaqus Analysis User's Guide. Dassault Systèmes: Vélizy-Villacoublay, France; 2014.
- [31] Shiradhonkar SR, Sinha R. Maximum and residual flexural crack width estimation in reinforced concrete frame members under seismic excitation. *J Struct Eng* 2018; 144(8):04018121.
- [32] Csi C. Analysis reference manual for SAP2000, ETABS, and SAFE. Computers and Structures, Berkeley, California, USA; 2016.